SUPPLEMENTAL ANNEX

CONCENTRATING SOLAR POWER IN CHINA AND INDIA:

A SPATIAL ANALYSIS OF TECHNICAL POTENTIAL AND THE COST OF DEPLOYMENT

Kevin Ummel[♀]

Version date: July 5, 2010

Overlay analysis

After identifying candidate cells at ~300m resolution (GlobCover), a 2km exclusionary safety buffer was applied to neighboring cells containing water, evidence of occasional flooding, permanent ice or snow, or artificial surfaces. A consolidation algorithm was then applied to ensure that only contiguous fields sufficient for operation of at least 100MW parabolic trough plant were retained. The results were aggregated to 30-arc-second (~1km) resolution summing the total area of candidate cells. Geomorphologcal safety buffers consisted of 8km for sand dunes and 2km for all other potentially problematic features. Solar radiation data were bilinearly downscaled from original ~40km resolution to ~10km resolution for estimation of capacity factor and levelized cost. Results were then downscaled to ~1km and the results of the overlay analysis were applied to identify final potential CSP area.

The final data product consists of estimated, annual CSP electricity production and a relative LCOE index for all suitable terrain at a resolution of ~1km.

Modeling plant performance

Forty global locales thought to be representative of potential CSP sites were identified from a sample of 2,000 weather stations by first restricting to stations with average daily DNR greater than 4.7 kWh per m^2 and then using a clustering algorithm to select representative sites on the basis of radiation profile and distance from the equator. Detailed modeling in SAM was performed for these sites, and the results were used to construct the regressions in Figures A1 and A2.

The levelized cost index is derived from modeling results using SAM's default cost estimates. Actual costs of CSP construction in China and India may be quite different from the SAM defaults but assuming the ratio of array to power block costs is roughly similar, the index will accurately reflect *relative* differences in LCOE across space.

[♀] MESPOM candidate; School of Earth, Atmospheric, and Environmental Sciences; University of Manchester
Contact address: publications@cgdev.org

The main text can be downloaded at: http://www.cgdev.org/content/publications/detail/1424287

Figures A1 and A2: Graphical regression results for estimated capacity factor and levelized cost index

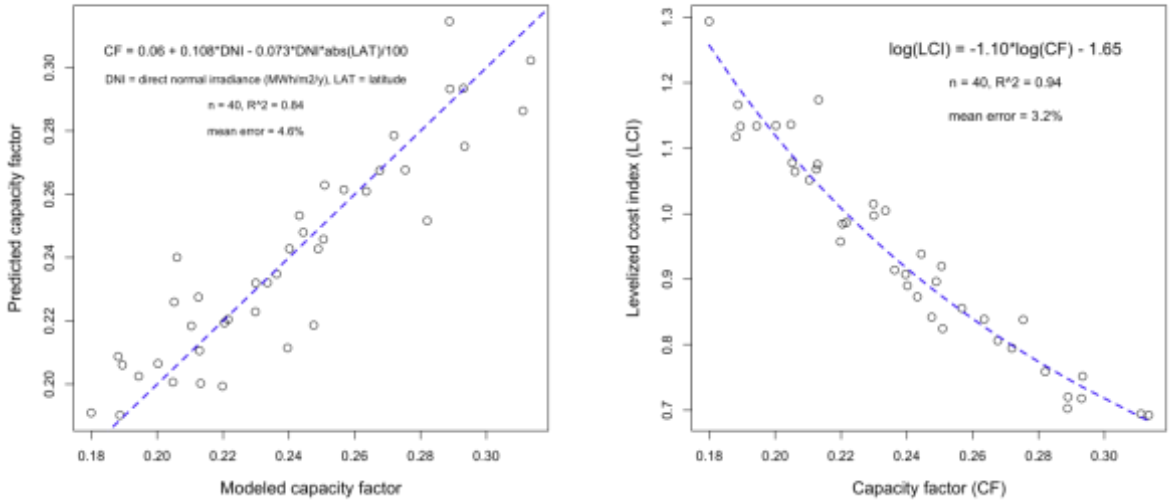

The "reference" DNI value is a user-specified input to SAM that determines the size of the solar field for a given solar multiple. A good estimate is the maximum hourly DNI incident on the solar field during the year, which can be approximated given hourly DNI and latitude. Following the SAM convention and assuming a flat solar field, the reference value was calculated for each of the representative sites:

$$D = 0.409 \sin\left[\frac{2\pi(284+n)}{365.25}\right] \qquad H = \frac{\pi(12-h)}{12} \qquad A = \sin^{-1}\left[\sin(D)\sin(l) + \cos(D)\cos(H)\cos(l)\right]$$

$$Z = \begin{cases} \pi - \cos^{-1}\left[\dfrac{\cos(D)\sin(l)\cos(H) - \sin(D)\cos(l)}{\cos(A)}\right], & if\ 0 < H < 12 \\ \pi + \cos^{-1}\left[\dfrac{\cos(D)\sin(l)\cos(H) - \sin(D)\cos(l)}{\cos(A)}\right], & if\ 12 < H < 24 \\ \pi, & if\ H = 12 \\ 0, & if\ H = 0 \end{cases}$$

$$I = R\sqrt{1 - \left[\cos(A) - \cos(A)\left[1 - \cos(Z)\right]\right]^2}$$

where all angles are in radians, *n* is day of the year, *h* is solar time, *l* is site latitude, *H* is hour angle, *A* is solar altitude, *Z* is solar azimuth, *R* is direct normal radiation, and *I* is incident radiation on the solar field.

Generation and transmission cost assumptions

The upper-bound cost estimate for CSP assumes: total capital costs of $3,577 per kW, annual operation and maintenance equal to 3% of capital cost, capacity factor of 25%, operating life of 30 years, 10% discount rate, 7% interest rate, and 50% debt fraction. Debt service is constant over 20 years. Capital and operating costs are taken from Williges et al. (2010).

The reference cost for supercritical coal assumes: total capital costs of $600 per kW, annual operation and maintenance of $4.60 per MWh, capacity factor of 90%, operating life of 30 years, 10% discount rate, 7% interest rate, 70% debt fraction, and net thermal efficiency of 40.3%. The energy content of coal is assumed to be 23 MJ per kg. Capital cost is taken from Chen and Xu (2010).

The additional cost of CSP-grid integration is assumed to consist of a transmission and load-balancing component. The transmission component varies with distance and is estimated from modeling of plant and transmission infrastructure costs taking into account line and converter losses, using values reported elsewhere (Ummel and Wheeler 2008, Trieb et al. 2009, Williges et al. 2010).

Studies of wind power utilization within existing grids find that the additional cost of load balancing is typically less than 10% of the wholesale cost of power at penetration rates up to 20% (Holttinen et al 2007; Strbac et al. 2007; DOE 2008). Modeling of CSP with hybrid gas generation results in negligible costs of intermittency and balancing up to penetration rates of ~40% (Zhang and Smith 2008). In light of this evidence, a baseline markup of 5% is included alongside transmission costs. Figure A3 shows the combined, assumed increase in levelized cost and line and conversion losses for a given distance from CSP supply to final consumption. Coal is assumed to face no additional transmission or balancing charges.

Figure A3: Estimated increase in CSP cost and line and conversion losses with transmission distance

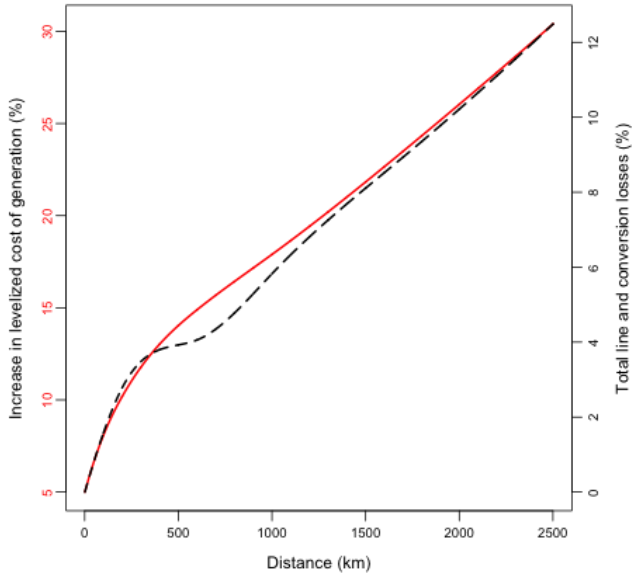

Estimating spatial distribution of power supply

Nighttime lights data were used to allocate domestic power supply in 2007 across all grid cells in the country at ~1 km resolution (NOAA 2009). The digital number (DN) for light magnitude ranges from 0 to 63, but saturation is known to occur in densely populated areas. A natural spline function, adapted from the technique of Letu et al. (2009), was fit to the rank-ordered DN values for 0<DN<55, beyond which extrapolated values were used (corrected values ranged up to ~70).

Power supply (S) in each cell (i) was initially estimated as: $S_i = T\frac{DN_i}{\sum DN}$, where T is total domestic supply before distribution losses (IEA 2009). As a quality-check on the allocation procedure, the estimates of S_i were summed at the provincial level and compared to official data (CEA 2008; NBSC 2009). Figures A4 and A5 report the results, which show relatively high correlation and suggest corrected DN is a reasonable predictor of the spatial distribution of national supply. Initial grid cell estimates were

then adjusted by the ratio of the actual (*a*) to estimated (*e*) total for the relevant province (*p*) to give a final (*f*) estimate for the present distribution: $S_f = S_i \frac{\sum_p S_a}{\sum_p S_e}$

Figures A4 and A5: Actual and estimated provincial power supply in China (left) and India (right)

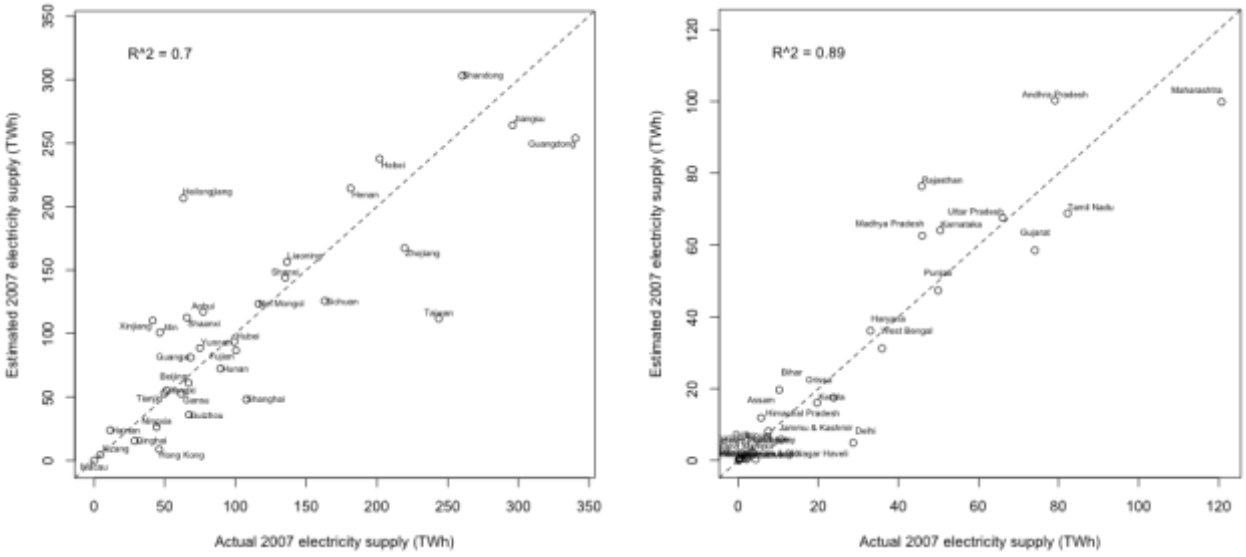

A similar approach to used to transform the present-day estimates into future projections. The 2025 spatial population projection of Hachadoorian et al. (2007) is proportionally adjusted so that the country total matches the medium variant UN population projection. For each grid cell, the ratio of the corrected 2025 projection to present population total is used to scale up S_f. The country total for power generation is then proportionally adjusted again to match the 2025 reference case projection from the IEA (2009). This is akin to keeping per capita consumption constant and adjusting only for population increases – clearly unrealistic, but sufficient for the purposes here.

Spatial simulation of transmission

The transmission simulation uses ~50km resolution grid cells obtained by aggregating ~1km datasets for power consumption, CSP output, and levelized cost. This eases computation time and more realistically and effectively allows for short-distance transmission (~25km) to and from converter stations. This is only meant to approximate general trends in transmission requirements, not provide a detailed assessment.

The algorithm proceeds as describes in the main text. Constraints include a maximum transmission distance of approximately 2,500 km. Transmission at distances greater than 500 km is only allowed if a sufficiently large quantity of power is to be moved: >500 km requires >500 MW power; >1500 km requires >1500 MW power. The thresholds are based on review of existing and planned HVDC lines around the world.

Expansion program assumptions

The Sino-Indian CSP expansion program meets the total power deployment assumptions in Figure A6. The cost reductions over time are assumed to apply to the total levelized cost of delivered electricity, which includes transmission. Consequently, the cost reductions through learning effectively apply to both CSP construction and operation and transmission infrastructure.

The learning rate uses the *total* CSP deployment in both countries to calculate the expected cost reduction at each time step and uses an assumed starting capacity of 2,000 MW (the approximate total of global CSP in operation or under construction). The percent reduction in the CSP cost index value due to learning at any time (t) is given by:

$1-\left(\frac{C_t}{C_0}\right)^{\frac{\log(\alpha)}{\log(2)}}$, where C_t is total capacity, C_0 is the starting capacity (2 GW) and α is the learning rate.

Figure A6: Assumed deployment schedule for CSP expansion program

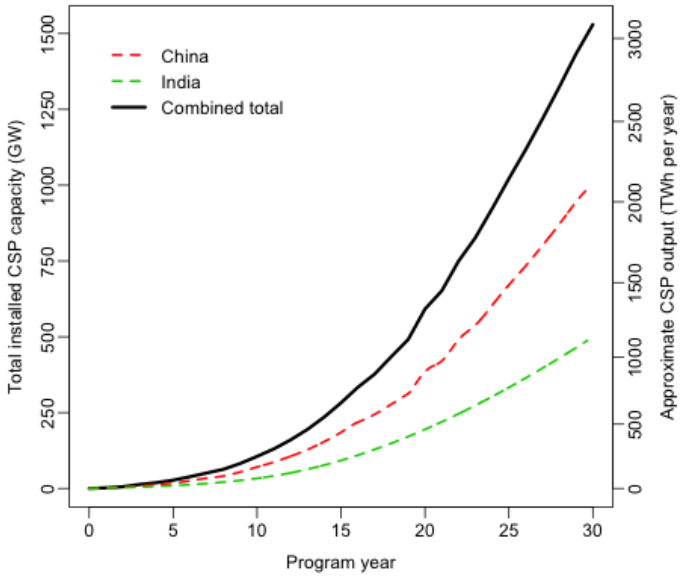

Additional figures and tables

Figure A7: Probability distribution and weighted mean of published wind power learning rates

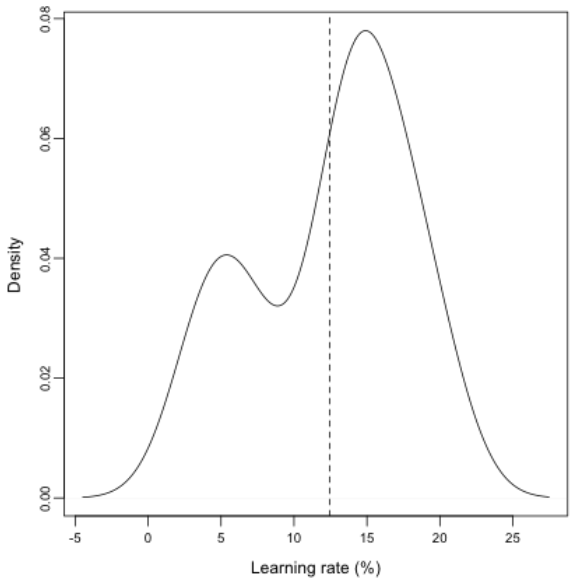

Table A8: Chinese CSP potential by region (area and potential power output)

China	**Scenario 1**	**Scenario 2**	**Scenario 3**
Nei Mongol	18,098 TWh/y	18,450	18,682
	258,240 km^2	263,330	266,789
Xinjiang	18,044	24,343	24,344
	249,827	325,686	325,705
Qinghai	6,994	10,015	10,024
	90,779	126,126	126,260
Tibet (Xizang)	5,188	15,118	15,121
	50,093	147,128	147,158
Gansu	2,696	3,392	3,400
	38,420	47,894	48,011
Others	114	144	288
	1,745	2,192	4,366
Totals	51,133 TWh/y	71,461	71,858
	689,103 km^2	912,356	918,290

Note: Totals may not sum due to rounding or omission of negligible figures.

Table A9: Indian CSP potential by state (potential power output and area)

India	**Scenario 1**	**Scenario 2**	**Scenario 3**
Rajasthan	2,221 TWh/y	2,320	2,389
	27,220 km^2	28,440	29,341
Jammu & Kashmir	69	115	116
	691	1,155	1,162
Gujarat	32	210	456
	431	2,816	6,075
Karnataka	~ 0	~ 0	162
			2,085
Madhya Pradesh	~ 0	~ 0	136
			1,816
Others	~ 0	~ 0	75
			997
Totals	2,324 TWh/y	2,648	3,334
	28,364 km^2	32,432	41,476

Note: Totals may not sum due to rounding or omission of negligible figures.

Figures A10 and A11: Insets of Changchun (China) and Bangalore (India) areas

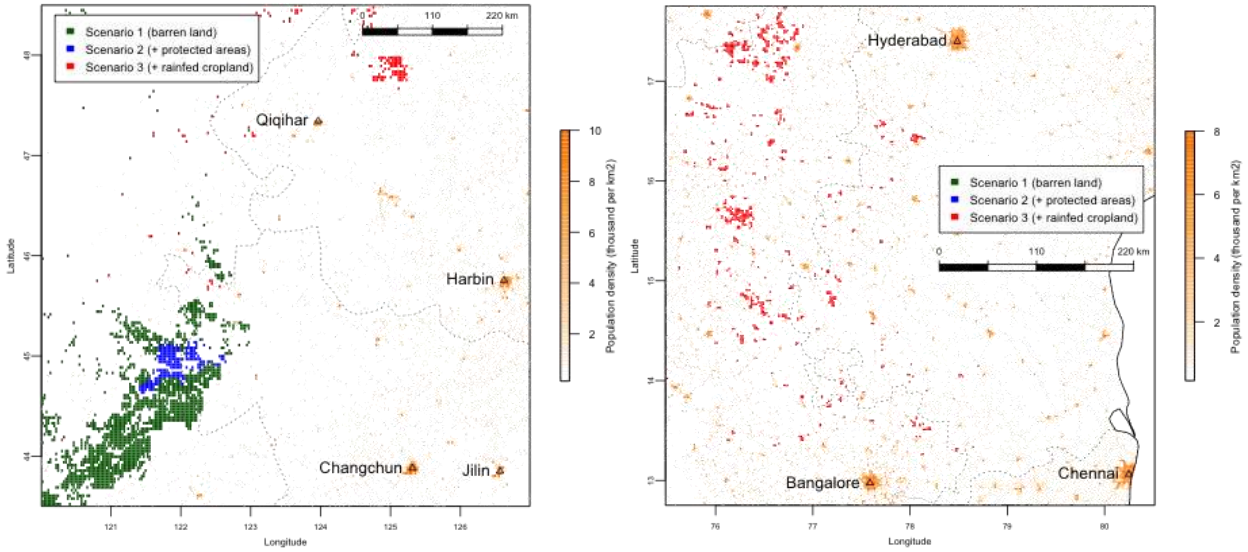

Figures A12 and A13: Proximity of select cities to CSP potential in China (left) and India (right) under Scenario 3

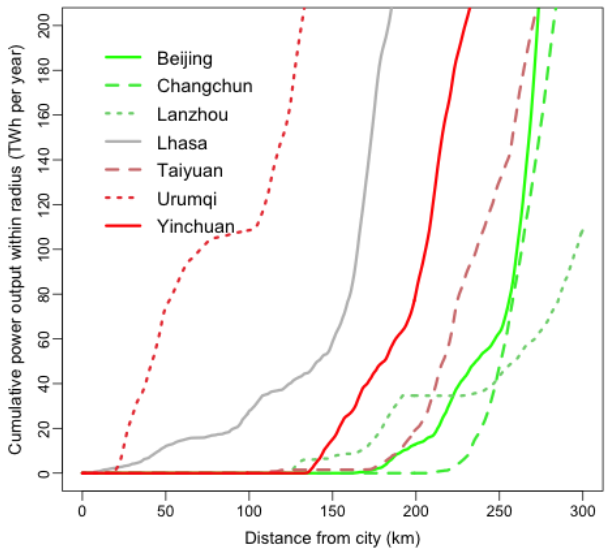

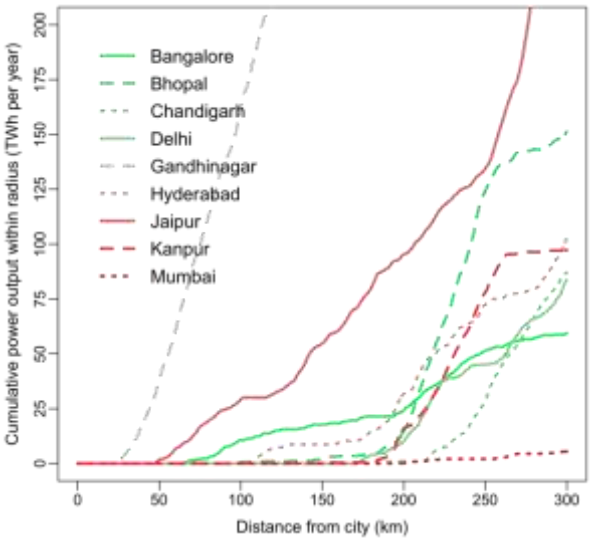

Figure A14 and A15: Distance and output under transmission simulation in China (left) and India (right)

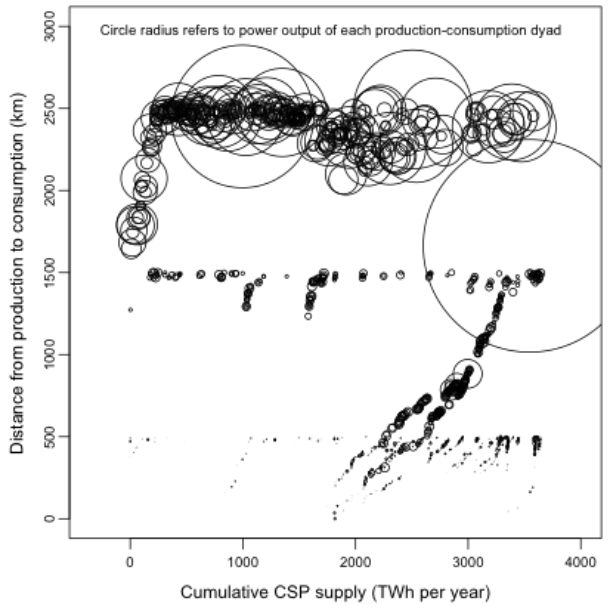

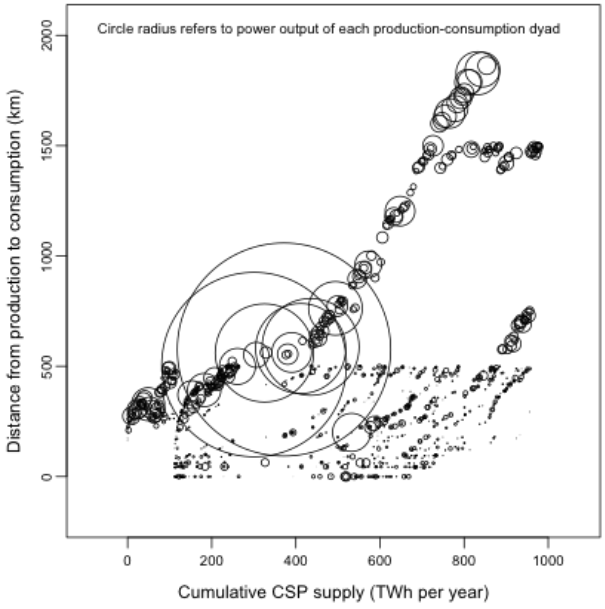

Figures A16 and A17: Expansion program results for China (15% learning rate, 7% discount rate)

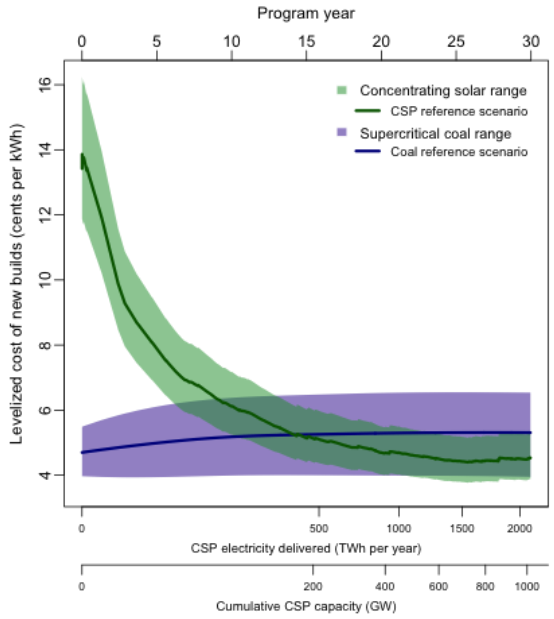

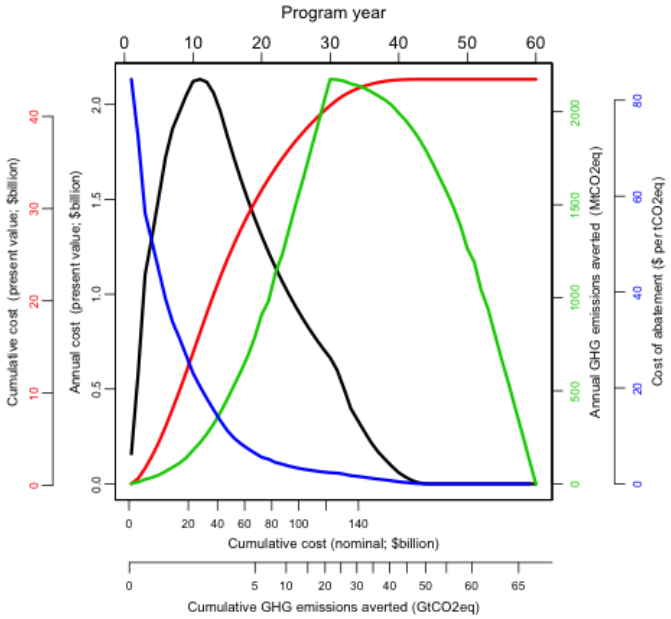

Figures A18 and A19: Expansion program results for India (15% learning rate, 7% discount rate)

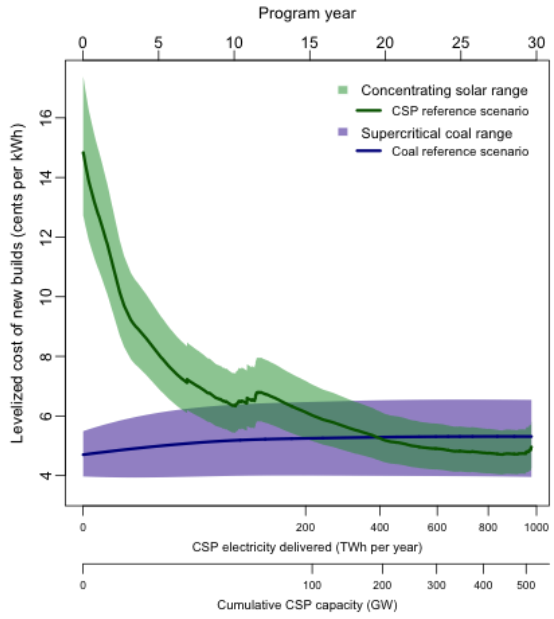

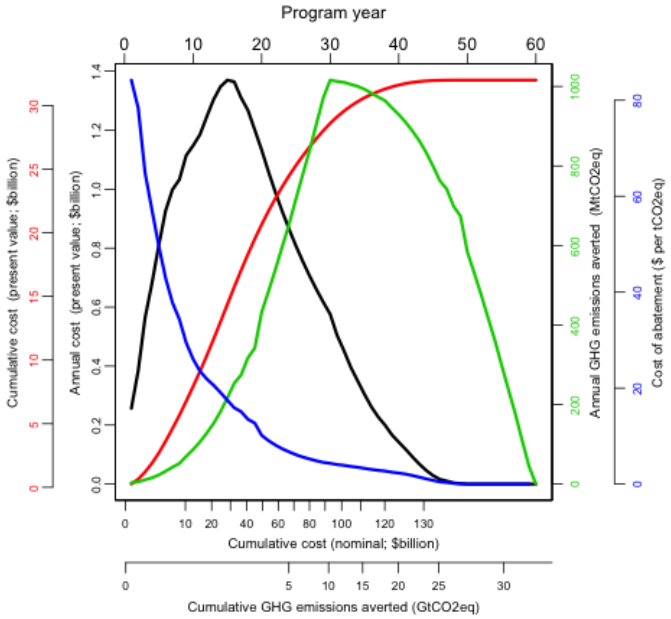

References

DOE. 2008. 20% wind energy by 2030: increasing wind energy's contribution to U.S. electricity supply. U.S. Department of Energy, DOE/GO-102008-2567, July.

Chen, W. and Xu, R. 2010. Clean coal technology development in China. *Energy Policy* 38 (5): 2123-2130.

CEA. 2008. 2007-2008 Annual Report. Central Electricity Authority, Ministry of Power, Government of India, July. Accessed 24 April 2010. Available at: http://www.cea.nic.in/about_us/annualreport.htm

Hachadoorian, L., Gaffin, S.R. and Engleman, R. 2007. Projecting a gridded population of the world using ratio methods of trend extrapolation. In *Human Population: The Demography and Geography of Homo Sapiens and their Implications for Biological Diversity*, eds. R.P. Cincotta, L. Gorenflo and D. Mageean. Berlin: Springer-Verlag.

Holttinen, H., Meibom, P., Ensslin, C., Hofmann, L., Tuohy, A., Tande, J.O., Estanquerio, A., Gomez, E., Söder, A., Shakoor, A., Smith, J.C., Parsons, B., and van Hulle, F. 2007. State-of-the-art design and operation of power systems with large amounts of wind power, summary of IEA wind collaboration. Presented at European Wind Energy Conference, 7-10 May, Milan, Italy.

IEA. 2009. World energy outlook 2009. International Energy Agency, Paris.

Letu, H., Hara, M., Yagi, H., Tana, G., and Nishio, F. 2009. Estimating the energy consumption with nighttime city light from the DMSP/OLS imagery. Presented at Urban Remote Sensing Joint Event, 20-22 May, Shanghai, China.

NBSC. 2009. China statistical yearbook 2009. National Bureau of Statistics of China.

NOAA. 2009. DMSP-OLS nighttime lights time series (1992-2008). Image and data processed by the National Oceanic and Atmospheric Administration's National Geophysical Data Center; DMSP data collected by U.S. Air Force Weather Agency. Available at: http://www.ngdc.noaa.gov/dmsp/downloadV4composites.html

Strbac, G., Shakoor, A., Black, M., Pudjianto, D. and Bopp, T. 2007. Impact of wind generation on the operation and development of the UK electricity systems. *Electric Power Systems Research* 77 (9): 1214-1227.

Trieb, F., O'Sullivan, M., Pregger, T., Schillings, C. and Krewitt, W. 2009. Characterisation of solar electricity import corridors from MENA to Europe. German Aerospace Center (DLR), Institute of Technical Thermodynamics, Stuttgart, Germany.

Ummel, K. and Wheeler, D. 2008. Desert power: the economics of solar thermal electricity for Europe, North Africa, and the Middle East. Working Paper No. 156, Center for Global Development, Washington, D.C.

Williges, K., Lilliestam, J. and Patt, A. 2010. Making concentrated solar power competitive with coal: the costs of a European feed-in tariff. *Energy Policy* 38 (6): 3089-3097.

Zhang, Y. and Smith, S.J. 2008. Long-term modeling of solar energy: analysis of concentrating solar power (CSP) and PV technologies. Pacific Northwest National Laboratory, prepared for U.S. Department of Energy.